

COMPACT TUNABLE HYPERSPECTRAL IMAGING SYSTEM

Phuong-Ha Cu-Nguyen¹, Adrian Grewe², Csaba Endrödy³, Stefan Sinzinger², Hans Zappe¹, and Andreas Seifert¹

¹Department of Microsystems Engineering – IMTEK, University of Freiburg, Germany

²Optical Engineering, Ilmenau University of Technology, Germany

³Micromechanical Systems, Ilmenau University of Technology, Germany

ABSTRACT

We present a compact hyperspectral imaging system consisting of a combined refractive-diffractive optical element for extended longitudinal chromatic aberration, which provides spectrally resolved information of an object. This fully integrated hybrid device features a diffractive optical element (DOE) acting as a positive lens, a tunable concave liquid-filled membrane lens, and integrated magnetic actuation for hydraulically tuning the focal length of the membrane lens. The lens system is demonstrated to generate a hyperspectral data cube in the visible wavelength range by imaging the light from a pinhole array in a confocal approach onto a CCD camera.

INTRODUCTION

Hyperspectral imaging is similar to spatially resolved spectroscopy of a reflecting object where a complete optical spectrum can be acquired at any position of an object within a short time. Due to its suitability and commercial availability, it has been implemented and established in very diverse applications as a detection method. The traditional approach to generate hyperspectral images is push broom scanning, commonly used in satellite cameras for earth observations from space. A push broom sensor employs a slit aperture scanning along the object. Each column of the image is laterally dispersed, using a prism, and imaged onto a detecting area, where the rows contain the spectral information [1].

An alternative approach is to spread and separate the spectral components of the light beam along the optical axis, for example by increasing the longitudinal chromatic aberration (LCA) of a lens system. By this way, a polychromatic or white light point source is spread into multiple points along the optical axis, and each point contains a spectral component with a certain band width of the light source. By using a pinhole in the image plane in front of the detector, only those wavelengths which focus directly onto the pinhole can pass the aperture and reach the detector area while other wavelengths are blocked. This approach, known as chromatic confocal microscopy, offers the maximum intensity for the wavelength to be detected, and has been introduced and implemented previously [2, 3, 4].

We present here a novel extension of chromatic confocal microscopy with an adaptive tunable optical system for hyperspectral image sensing. The main component is a compact hyperchromatic lens module which is realized by the combination of a DOE and a tunable liquid-filled membrane-lens. The lens system is equipped with a fully

integrated magnetic actuator and was fabricated by a low cost manufacturing method, yielding a flexible and fast operating system.

OPTICAL PRINCIPLE

The core of our presented system is a tunable hyperchromatic lens consisting of a DOE, acting as a positive lens, and a tunable refractive concave lens. This refractive-diffractive combination allows the lens system to have positive refractive power with maximized LCA. As a result, the light originating from an object point is transmitted through the system and the focal points of different wavelengths are distributed along the optical axis in the conjugated wavelength-dependent image planes. The confocal concept is implemented by inserting a pinhole in the optical path of the ray, functioning as a spatial filter, which allows the selected wavelength to cross the pinhole while blocking the others. By changing the focal length of the refractive lens, different wavelengths can traverse the pinhole and reach the detector.

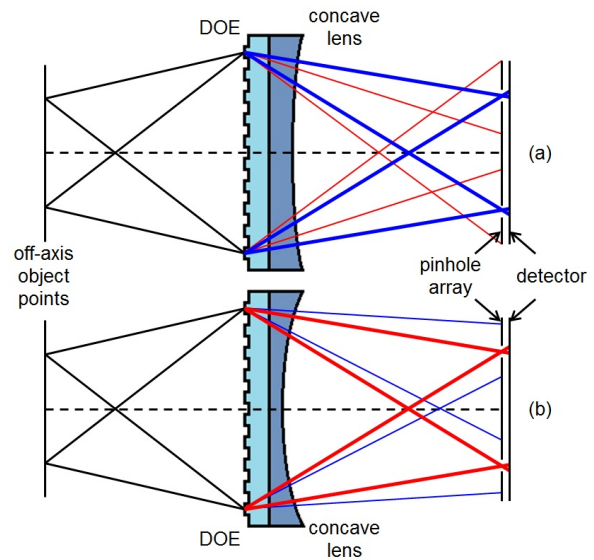


Figure 1: Schematic drawing of a hyperchromatic lens with off-axis multi-point hyperspectral sensing. By changing the curvature of the liquid lens, different spectral components from the object points are focused in the image plane. (a) Blue in focus; (b) red in focus.

We have shown previously that this lens system allows wavelength scanning for an on-axis point source over a large

spectral wavelength range from 450 to 900 nm, thereby providing narrow bands with spectral widths below 15 nm [5].

Adopting the same concept, an off-axis point source array is now employed for two-dimensional hyperspectral sensing, as sketched in Figure 1. The idea is realized by generating an array of point sources in the object plane of the lens system and a pinhole array directly before the detector in the image plane. All wavelengths which are out of focus and blurring the image are filtered out by the pinhole array so that a two-dimensional image of narrow spectral bandwidth can be generated. By changing the curvature of the concave lens, images of different wavelengths are formed in the image plane on the detector. For example, in Figure 1(a) the blue light emerging from the object point sources generates the image, whereas in Figure 1(b) the image contains the information of red light from the object.

STRUCTURE OF THE HYBRID LENS

The layout of the integrated hyperchromatic lens, including the electromagnetic actuator, is shown in Figure 2. The lens system consists of two chambers: one is the reservoir volume for the actuator while the other one is the optical cavity of the liquid-filled membrane-lens. The two chambers are connected by a channel, sealed with a polymeric membrane, and filled with DI water with a refractive index of 1.33.

When a current is applied to the coil of the electromagnet, an induced repulsive force is generated to push the magnet upwards, hence pulling the optical liquid from the lens chamber and thereby causing a concave deformation of the lens' membrane and thus a change in focal length. Depending on the amplitude of the current, the focal length can be tuned in a wide range with the resolution defined by the accuracy of the current source.

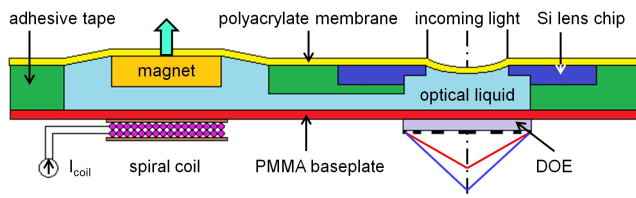


Figure 2: Layout of the hyperchromatic lens with integrated electromagnetic actuation scheme, a positive DOE and a deformable concave lens.

FABRICATION PROCESS

We developed a flexible, low cost fabrication process for the lens system. A summary of the process is given by the assembly steps outlined in Figure 3. The solid supporting structure of the fluidic lens and actuation scheme is made from the high performance adhesive transfer tape 3M™467MP 200MP. The tape was patterned by a CO₂ laser and stacked together to form the frame structure and alignment posts.

The essential elements of the system, including the Si lens chip and DOE, are fabricated by precise photolitho-

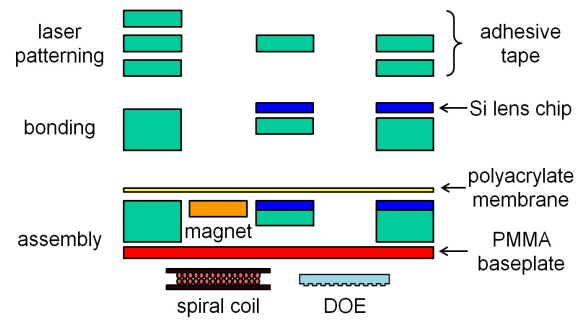


Figure 3: Process chart for assembling the hyperchromatic lens with integrated electromagnetic actuator.

graphic processes. The Si lens chip was fabricated by standard Si bulk micromachining including KOH etching from the back side and DRIE (deep reactive ion etching) from the front side to form a circular aperture of 3 mm.

The DOE was designed as a Fresnel zone plate with a focal length of $f_0 = 20$ mm at a wavelength of 550 nm, diffraction limited on the optical axis, and optimized for low spherical aberration. It is produced on quartz glass, fabricated by 2-step lithography using ICP-RIE etching, thereby forming a 4-level structure.

The actuator consists of a permanent NdFeB magnet, with a residual magnetization of 1.17 – 1.21 T, attached on the polymeric membrane inside the actuating cavity, and driven by the magnetic field of a spiral coil with 500 windings of 100 μ m copper wire and inductance of 3 mH, which is bonded on the PMMA baseplate outside the actuation cavity.

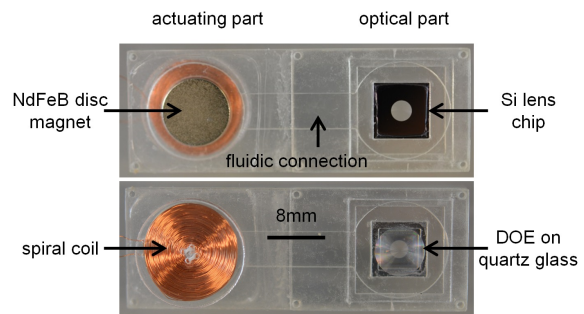


Figure 4: Photo of the back and front of the assembled hyperchromatic lens with integrated electromagnetic actuator.

Stacking and assembling of the lens components was performed with the aid of the integrated alignment structures. On the top and bottom of the solid frame are precise square posts which define the position of the diced Si lens chips and the DOE and allow precisely aligned mounting.

The optical aperture and actuating cavity were covered by a polyacrylate membrane (3M™VHB™4905) [6]. The whole frame was bonded onto a 350 μ m thick PMMA baseplate and the cavity was filled with DI water. A complete prototype of the tunable hyperchromatic lens was assembled and is shown in Figure 4.

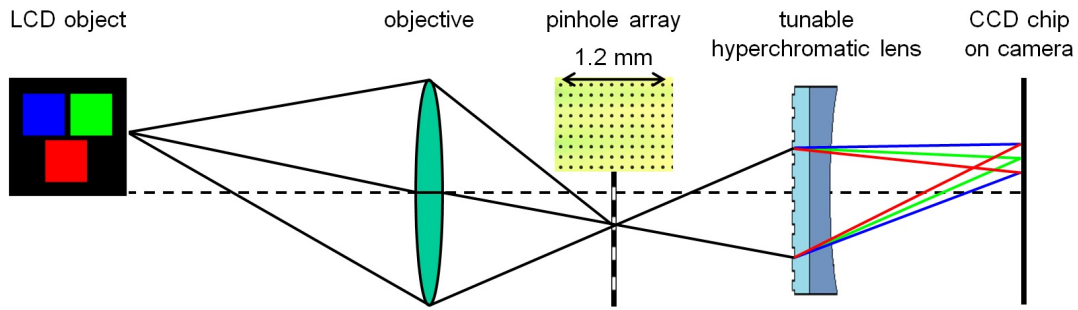


Figure 5: Schematic of the measurement setup for off-axis hyperspectral sensing. The object to be imaged is a colored pattern on an LCD screen. Based on the actuation current of the tunable lens module and the arrangement of the optical components, the spectral information of the object can be extracted on the CCD chip.

MEASUREMENT SETUP

To characterize the hyperspectral module, the measurement setup shown in Figure 5 was employed. To demonstrate the functionality of the system, colored rectangular areas with RGB values of 255 for either red, green or blue on an LCD monitor were taken as the object. This LCD object is first imaged into an intermediate image plane, where we place a pinhole array with hole diameters of $40\ \mu\text{m}$ at a spacing of $120\ \mu\text{m}$ to generate the array of point sources as the object for the hyperchromatic lens.

The intermediate image covers an area of $1.2\ \text{by}\ 1.2\ \text{mm}^2$ on the pinhole array and forms an object consisting of $11\ \text{by}\ 11$ measuring points. From each of these point sources, a ray bundle originates with the spectral information of conjugated points in the original object plane. The array of object points is imaged by the hyperchromatic lens onto the CCD chip of the camera. The pinhole array before the detector is virtually simulated by an appropriate choice of the pixels on the CCD. The hyperchromatic lens is used in a $4f$ setup with equal object and image distance of $52\ \text{mm}$, yielding an angle of view of 1.32° , hence off-axis aberrations can be neglected.

RESULTS AND DISCUSSION

The change in focal length of the hyperchromatic lens by tuning the current of the actuating coil is the basic principle of the wavelength scanning process. In the image plane, only specific wavelengths with the focal length defined by the object and image distances as well as the actuating current can generate a sharp image of the object points.

The intensity of the wavelength, assigned by the actuation setting, can be determined by measuring the gray scale intensity of the sharply imaged points. For evaluating the intensity of the CCD images, circular areas with the size of the pinhole ($40\ \mu\text{m}$) were taken. The chosen diameter ensures that no overlap between adjacent points appears and out-of-focus wavelengths are filtered out as far as possible. Choosing a smaller diameter would deliver a better spectral resolution but only at the cost of considerably reduced intensity. The spectral bandwidth of the light from a sharply imaged point was previously measured with a value of about $13\ \text{nm}$ [5].

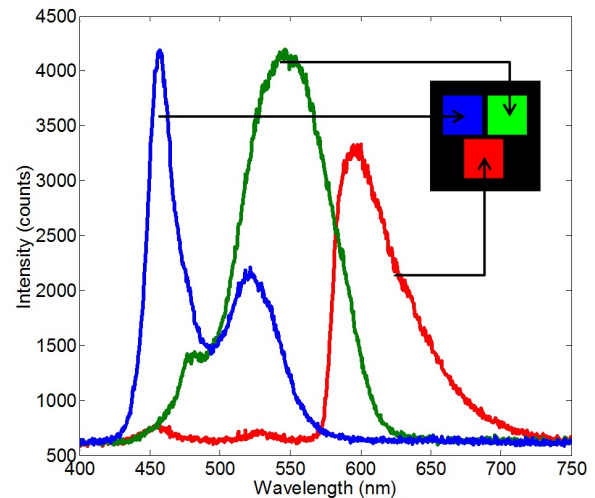


Figure 6: Reference spectra of three RGB areas of the object, recorded by an optical spectrum analyzer.

By changing the current over a wide range from 1 to $140\ \text{mA}$ with a resolution of $1\ \text{mA}$, a spectral tuning over the full visible range of $400\text{--}730\ \text{nm}$ is realized, thus forming a three-dimensional $11 \times 11 \times 140$ hyperspectral data cube.

The spectra of the R, G & B squares on the object are shown in Figure 6 and were measured by a commercial optical spectrometer directly in front of the LCD screen as a reference. Figure 7 shows the intensity variations of three arbitrary points of the object indicated by the arrows. The intensities were measured in terms of gray scale values on the CCD camera when the hyperchromatic lens was actuated by increasing the coil current. It was demonstrated earlier [5] that the correlation between wavelength and coil current was highly linear; therefore the intensity is plotted as a function of the coil current and corresponding wavelength.

When we compare the peak positions of the CCD-based measurement with the peaks of the spectrometer-based reference measurement, we see excellent agreement. The amplitude differences can be explained by different spectral sensitivities of the spectrometer and the CCD chip, and by the impact of the hyperspectral lens, i.e. for example the

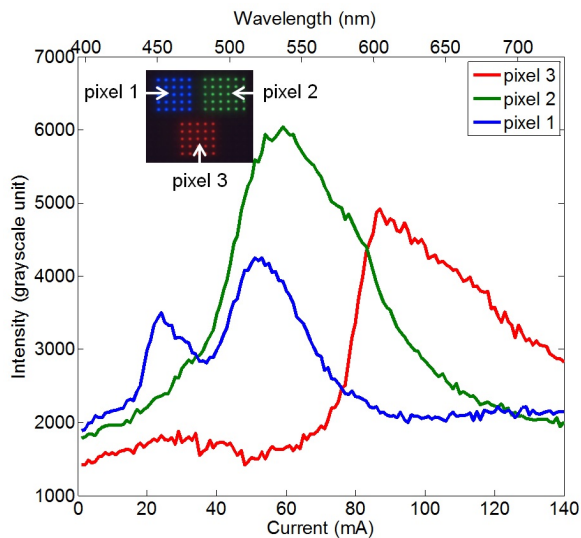


Figure 7: Intensity in terms of gray scale values for the R, G and B “pixels” imaged and measured on the CCD camera as a function of coil current and related wavelength.

wavelength-dependent diffraction efficiency of the DOE, on the CCD-based measurement.

Figure 8 displays eight of the 140 hyperspectral images of the entire object obtained on the CCD chip, corresponding to 8 actuation states. Each image delivers a specific wavelength information of the object. The series of images shows that two-dimensional images of narrow spectral bandwidth can be generated over the entire visible spectral range.

The images reveal that out-of-focus wavelengths contribute to the spectral information of the image as blurred rings around the sharp points, albeit with a strong decay due to the longitudinal chromatic aberration. Accordingly, the spacing of the pinhole array was chosen to avoid cross-talk between adjacent points. As a result, the spatial information of the object is affected and the spatial resolution is reduced. This can be improved by laterally moving the pinhole array in both directions to fill the gaps between the pinholes.

CONCLUSION

A compact tunable hyperchromatic lens for imaging a two-dimensional object with highly resolved spectral information was established. The fully integrated hybrid device was demonstrated to generate a hyperspectral data cube in the visible wavelength range of 400–730 nm with a spectral sampling interval of 2.4 nm. The spectra of the image points derived from the hyperspectral images are in good agreement with reference measurements from a spectrometer, measuring the spectral properties of the object directly. Due to the confocal principle of the system, realized by a pinhole array in an intermediate image plane, reduced lateral information and resolution compared to full-field imaging results. An improved system will feature a 2D electrostatically movable pinhole array to improve the spatial resolution. Pinhole diameter and spacing will be optimized

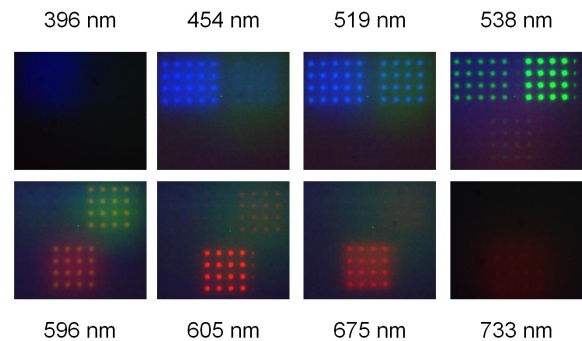


Figure 8: Eight of the 140 hyperspectral images acquired on the CCD camera during the scanning process for coil currents ranging from 1 to 140 mA. The corresponding wavelengths are specified in the figure.

in the same context to enhance the hyperspectral features of the developed system.

ACKNOWLEDGEMENT

This work is supported by the German Federal Ministry of Education and Research BMBF in the project ‘Optical Microsystems for Ultra-compact Hyperspectral Sensors’ (OpMiSen, FZK 16SV5575K).

REFERENCES

- [1] P. Mouroulis and M. McKerns, “Pushbroom imaging spectrometer with high spectroscopic data fidelity: experimental demonstration,” *Opt. Eng.*, vol. 39, no. 3, pp. 808–816, 2000.
- [2] K. Koerner, C. Kohler, E. Papastathopoulos, A. Ruprecht, T. Wiesendanger, C. Pruss, and W. Osten, “Arrangement for rapid locally resolved flat surface spectroscopic analysis or imaging has flat raster array of pinholes turned about acute angle relative to spectral axis on detector matrix which fills up with elongated su-matrices,” Patent DE20 061 007 172, 2013.
- [3] M. Hillenbrand, A. Grewe, and S. Sinzinger, “Parallelized chromatic confocal systems enable efficient spectral information coding,” *Opt. Des. Eng., SPIE Newsroom*, DOI 10.1117/2.1201301.004642, 2013.
- [4] A. Grewe, M. Hillenbrand, and S. Sinzinger, “Hyperspectral imaging sensor systems using tunable lenses,” *Photonik 1/2013*, pp. 38–41, 2013.
- [5] P.-H. Cu-Nguyen, A. Grewe, M. Hillenbrand, S. Sinzinger, A. Seifert, and H. Zappe, “Tunable hyperchromatic lens system for confocal hyperspectral sensing,” *Opt. Express*, vol. 21, no. 23, pp. 27 611–27 621, 2013.
- [6] W. Zhang, H. Zappe, and A. Seifert, “Polyacrylate membranes for tunable liquid-filled microlenses,” *Opt. Eng.*, vol. 52, no. 4, pp. 046 601–046 601, 2013.